

## HYSTERESIS-CONTROLLED ACTIVE FILTER USING AN ARTIFICIAL NEURAL NETWORK FOR LINE HARMONIC SUPPRESSION

BARAKAM KARTHIK<sup>1</sup>, DR.P.SUJATHA<sup>2</sup>

<sup>1</sup>PG-Scholar, Department of EEE (Electrical Power Systems), JNTUA College of Engineering, Ananthapuramu, A.P., India

<sup>2</sup>Professor, Department of EEE, JNTUA College of Engineering, Ananthapuramu, A.P., India.

### Abstract:

This study introduces a thorough approach for developing a Active power filter with the goal of improving power quality in utility grids. The system utilizes an Artificial Neural Network (ANN) controller to effectively control the DC-link voltage. This is achieved by employing the Instantaneous Reactive Power Theory to extract the reference current. Hysteresis current control is used to generate gate pulses for regulating the switches of a Voltage Source Inverter (VSI). The system utilizes the Instantaneous Real and Reactive Power Theory (PQ theory) to monitor real and reactive powers and create reference currents accordingly. The simulation results show a considerable decrease in Total Harmonic Distortion (THD), suggesting that the proposed method effectively enhances power quality in utility systems.

**Keywords:** shunt Active Power Filter, Artificial Neural Network controller, Real and Reactive Power Theory

### 1.Introduction:

This study investigates how harmonics produced by non-linear loads affect the power

quality of the transmission and distribution systems. Harmonic distortion, voltage fluctuations, and noise are power quality issues that arise from non-linear loads, such as personal computers, variable frequency drives (VFDs), and arc furnaces [3,4,5]. Power losses, electric device heating, insulation failure, communication system interference, and, in the worst-case scenario, electric power system breakdowns can all be caused by harmonic distortion in low-voltage distribution systems [6,7]. In 1992 (IEEE Std 519-1992 [9]), amended in 2014 (IEEE Std 519-2014 [10]), the Institute of Electrical and Electronics Engineers—rules Association (IEEE-SA) established rules for harmonics restrictions in response to these problems. A total harmonic distortion (THD) of more than 5% is considered unacceptable according to these guidelines. Historically, power filters—especially passive ones—have been used to achieve this restriction. The scale, resonance, instability, and rigidity of industrial nonlinear loads coupled to stiff power supplies make it difficult to design an efficient passive power filter [19]. Proposed as a solution to the limitations of passive filters, active filters (AFs) employing have emerged. AFs present benefits such as enhanced filtering precision, swift dynamic response, and versatility [20,21]. The efficiency

of the shunt active power filter in reducing harmonics [22] is influenced by factors including the detection of current harmonics, measurement of reactive power, and the compensation control algorithm, all based on the theory of instantaneous reactive power.

is frequently used in control approaches for reference compensation current (P-Q theory). Several methods have been suggested by researchers for extracting both fundamental and harmonic components, establishing reference compensation currents, and controlling the voltage of the DC-link capacitor. For instance, an adapted version of P-Q theory was devised [24] to calculate reference compensation currents for mitigating harmonic currents. Methods such as reducing harmonic currents in voltage imbalances [25], removing harmonic distortion on the source side [26], managing the effect of harmonics on rectifier transformers [27], obtaining components with a positive sequence [28], and using a multilevel converter control strategy to eliminate harmonics [29] are among the other options. The literature review provides a strong foundation for our investigation by providing a range of studies on the control and design of shunt active power filters. Previous research has largely focused on improving the power quality of balanced power systems. Moreover, there is a limited number of published studies that tackle the design of Artificial Neural Networks (ANN) controllers for active filters (AFs).

However, this paper extensively outlines the methodologies through which a Simulink model of an ANN-based SAPF utilizes the

instantaneous reactive power theory to extract reference currents.

### 1. Topology and Operation of Active Shunt Filter

An Active Shunt Filter, depicted in Figure 1, comprises two primary circuits: the power circuit and the control circuit.

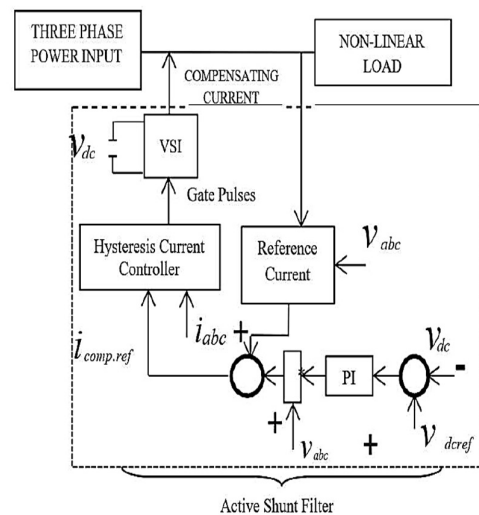


**Fig1: Simulation diagram of the Active Shunt Filter**

The power circuit needs to generate the necessary compensatory current. This circuit comprises a voltage source inverter (VSI) based on pulse-width modulation (PWM) to manage and regulate the DC voltage, alongside a DC-link capacitor for energy storage.

Simultaneously, the control circuit constantly tracks variations in harmonic currents to calculate the instantaneous reference compensation current. Based on this information, it fine-tunes the power circuit to accurately generate the needed harmonic current.

The Active Filter injects harmonic voltage (for series active filters) or current (for shunt active filters) in the opposite direction into the power

supply. Many methods for identifying and extracting harmonic currents have been researched and applied [7–10]. The methodologies encompass various approaches such as instantaneous real-reactive power (p-q) theory, adapted instantaneous p-q theory, neural networks [10], flux-based controllers, notch filters, and synchronous reference (d-q-0) theory. Despite demonstrating outstanding steady-state precision and fast response [6], p-q theory is found inadequate for estimating reference current in scenarios where the source voltage is suboptimal [6,11]. An analysis and simulation of an active shunt filter working under nonlinear load conditions are presented in this study.

## 2.1 DESCRIPTION OF P-Q THEORY:

Instantaneous power concepts are categorized into two main groups. One relies on the absolute phase with respect to three orthogonal axes, while the other is built directly on the a, b, and c phases. The transformation from a-b-c to  $\alpha$ - $\beta$ -0 establishes the former, referred to as the p-q hypothesis [5]. This approach is applicable to three-phase power systems with or without a neutral wire, capable of managing various voltage and current waveforms in both steady-state and transient conditions. Regulating active shunt filters in real-time becomes more straightforward with the application of this theory. Its straightforward calculations, predominantly algebraic, with the exception of distinguishing between the mean and alternate values of estimated power components, are another notable aspect. Each of these power components serves distinct functions.

P: The rate at which energy is transferred from the power source to the load through the a, b, and c phases is denoted by instantaneous average power. Instantaneous reactive power, or Q, represents the power that needs to be distributed among the three phases of a three-phase power system. Unlike active power, this current contributes to unwanted currents rather than facilitating energy transfer from the source to the load.

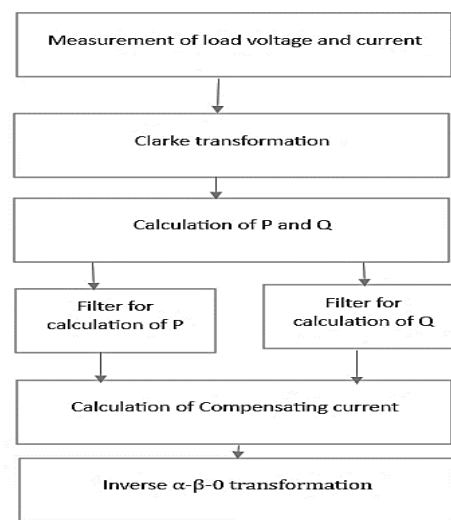


**Fig 2: PQ method control strategy**

The p-q theory employs an algebraic transformation known as the Clarke transformation to convert the three-phase voltages and currents, initially represented in the a-b-c coordinates, into the  $\alpha$ - $\beta$ -0 coordinates. Subsequently, the theory calculates the instantaneous power components. The conversion of the three-phase generic instantaneous line currents ( $i_a$ ,  $i_b$ , and  $i_c$ ) becomes simpler with the assistance of the  $\alpha$ - $\beta$ -0 axis.

$$\begin{bmatrix} V_0 \\ V_\alpha \\ V_\beta \end{bmatrix} = \sqrt{\frac{2}{3}} \begin{bmatrix} \frac{1}{\sqrt{2}} & \frac{1}{\sqrt{2}} & \frac{1}{\sqrt{2}} \\ 1 & -\frac{1}{\sqrt{2}} & -\frac{1}{\sqrt{2}} \\ 0 & \frac{\sqrt{3}}{2} & -\frac{\sqrt{3}}{2} \end{bmatrix} \begin{bmatrix} V_a \\ V_b \\ V_c \end{bmatrix} \quad \text{---(1)}$$

$$\begin{bmatrix} I_0 \\ I_\alpha \\ I_\beta \end{bmatrix} = \sqrt{\frac{2}{3}} \begin{bmatrix} \frac{1}{\sqrt{2}} & \frac{1}{\sqrt{2}} & \frac{1}{\sqrt{2}} \\ 0 & -\frac{1}{\sqrt{2}} & -\frac{1}{\sqrt{2}} \\ 0 & \frac{\sqrt{3}}{2} & -\frac{\sqrt{3}}{2} \end{bmatrix} \begin{bmatrix} I_a \\ I_b \\ I_c \end{bmatrix} \quad \text{---(2)}$$

The  $\alpha$ - $\beta$ -0 transformation serves to isolate the zero-sequence component from the a-b-c phase components, with the zero-sequence elements excluding contributions from the  $\alpha$  and  $\beta$  axes. Equations 1 and 2 allow for the calculation of the instantaneous real and imaginary power components on the source side.

$$\begin{bmatrix} p \\ q \end{bmatrix} = \begin{bmatrix} V_\alpha & V_\beta \\ -V_\beta & V_\alpha \end{bmatrix} \begin{bmatrix} I_\alpha \\ I_\beta \end{bmatrix} \quad \text{--- (3)}$$

Where:

$p = V_\alpha I_\alpha + V_\beta I_\beta$  Instantaneous Real Power

$q = V_\alpha I_\beta - V_\beta I_\alpha$  Instantaneous Imaginary Power

we can calculate reference current as

$$\begin{bmatrix} i_{fa}^* \\ i_{fb}^* \\ i_{fc}^* \end{bmatrix} = \sqrt{\frac{2}{3}} \begin{bmatrix} 1 & 0 \\ -\frac{1}{2} & \frac{\sqrt{3}}{2} \\ \frac{1}{2} & \frac{\sqrt{3}}{2} \end{bmatrix} \begin{bmatrix} I_\alpha \\ I_\beta \end{bmatrix} \quad \text{--- (4)}$$

The orientation of the  $\beta$  axis ensures that if spatial vectors representing voltage or current in the abc coordinates rotate in the abc sequence, they will similarly rotate in the  $\alpha$ - $\beta$  sequence on the  $\alpha$ - $\beta$  coordinates.

## 2.2. PI CONTROLLER:

Proportional and integral terms make up the PI controller. The response to the current error is governed by the proportional value, while the response based on the cumulative sum of past errors is governed by the integral. The DC link capacitor's voltage has been controlled using a PI controller. As an input to the PI controller, VDC is compared to VDC-ref in this technique to produce an error signal. The recommended error signal follows the reference current signal via the PI controller, which assisted in achieving zero steady state. To produce the necessary switching signals for the shunt APF switches, a hysteresis controller is used.

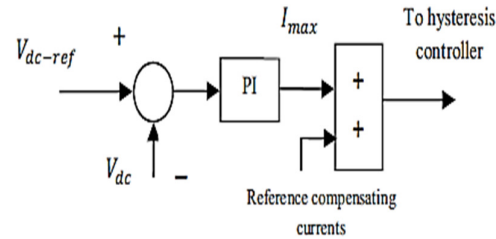


**Fig 3: DC link voltage Regulation**

## 2.3. Hysteresis-Current Controller:

The hysteresis current controller in the suggested method provides the precise gating pulse sequence of the IGBT-based VSI utilized in the proposed, as seen in the above image. The reference voltage or reference current available at the output of ANN controller is compared with the feedback voltage or current to generate the error signal. The hysteresis band comparator, which generates the gating signal needed by the AF, compares the error signal. AF generated the compensating current to mitigate the harmonic content.

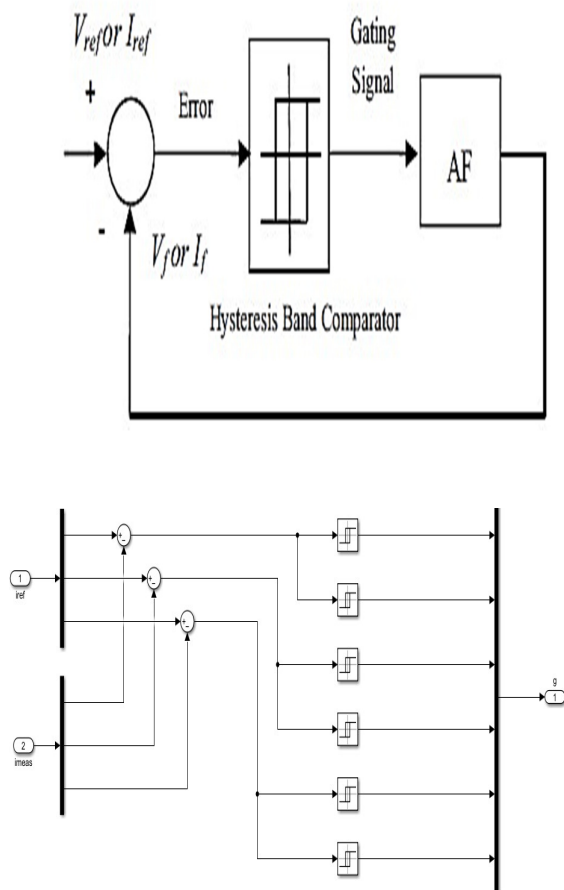


**Fig 4: Simulink diagram of Hysteresis control**

**2.4 ANN CONTROLLER:**

An artificial neural network is the most effective controller when it comes to quickly identifying corrupted signals. The parametric variation condition prevents the traditional controller from operating. It is a collection of neurons with adoption and learning capabilities. The proposed controller structure comprises several neural layers, featuring neurons in the input layer, twenty neurons in the hidden layer, and one neuron in the output layer.

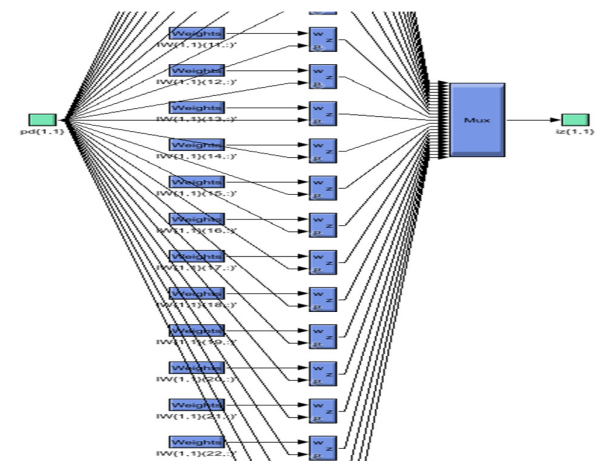
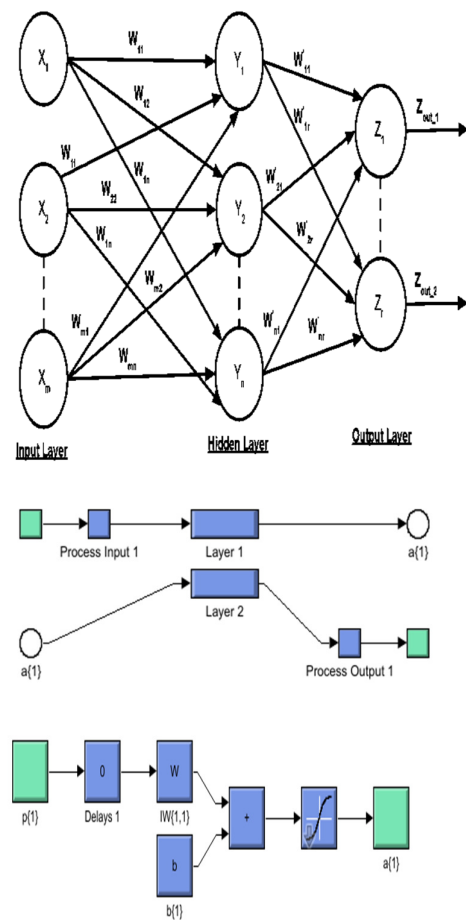


**Fig 5: Training process for ANN controller**

It undergoes training to acquire a reference signal. The output of the controller is then employed to generate the three-phase source

current reference, subsequently producing gating pulses for the APF switches.

### 3.Simulation Results:

#### A. With out ASF (Active shunt filter):

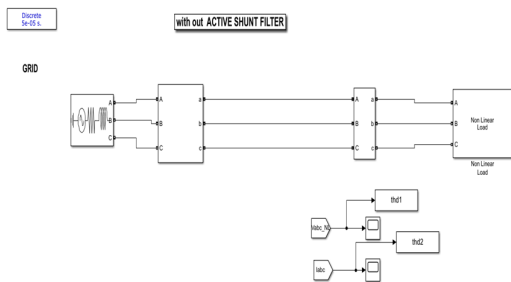


**Fig 6: Uncompensated Simulation model**

The Simulink model above depicts an Uncompensated Simulation model designed to simulate harmonics in the source voltage and current. The model includes a non-linear load, and it is evident that the source voltage contains harmonic components resulting from this non-linear load.

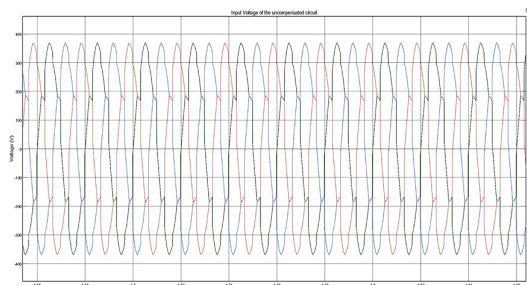


**Fig 7: Source voltage of Uncompensated circuit**

The graph above illustrates the distorted waveforms of the three-phase uncompensated source voltage and current within a balanced system featuring a nonlinear load. Through Fast Fourier Transform (FFT) analysis, it is demonstrated that the source voltage undergoes distortion because of the nonlinear characteristics of the load.

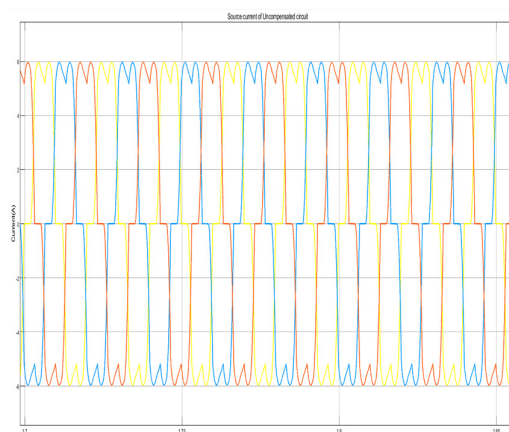


**Fig 8: Source current of Uncompensated circuit**

In the provided graph, the distorted waveforms of the three-phase uncompensated source voltage and current within a balanced system containing a nonlinear load are presented. Analysis conducted using the Fast Fourier Transform (FFT) reveals that the source current undergoes distortion as a consequence of the nonlinear characteristics exhibited by the load.

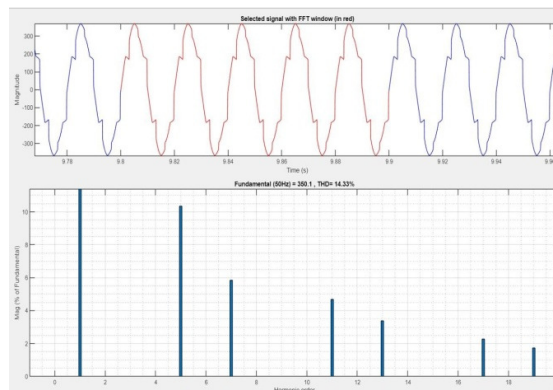


**Fig 9: THD of uncompensated source voltage waveform is 14.33%**

As indicated by the THD analysis presented above, distortion is observable in the waveforms of the three-phase source voltage and current within a balanced system featuring a nonlinear load. FFT analysis reveals that the nonlinear characteristics exhibited by the load result in distortion in the source voltage,

thereby contributing to a total harmonic distortion (THD) of 14.33% in the uncompensated source voltage. This level of harmonic distortion exceeds the permissible limits set by IEEE standards.

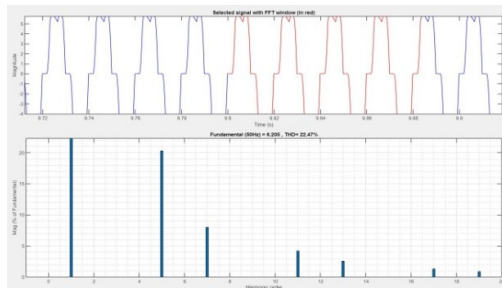


**Fig 10: THD of uncompensated source current waveform**

The earlier THD analysis illustrates distortion present in the waveforms of the three-phase source voltage and current within a balanced system featuring a nonlinear load. The distortion observed in the supply current is attributed to the nonlinear characteristics of the load. FFT analysis discloses a total harmonic distortion (THD) of 22.47% in the uncompensated source current, surpassing the thresholds outlined by IEEE standards.

**B. Compensated circuit (with PI-ASF)**

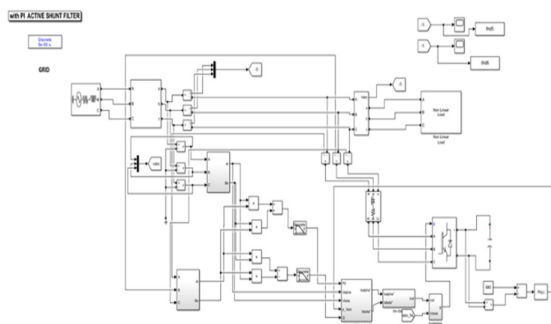


**Fig 11: Simulink Model with PI Active shunt filter**

The above figure represents simulation model of Shunt active filter using PI. One crucial aspect of regulating an active shunt filter is

maintaining a constant DC voltage on the voltage source inverter's side through intermediate circuit voltage regulation. These filters commonly include a capacitor to store energy. If there is little power flowing between the filter and the AC mains, the capacitor's voltage should remain constant. However, voltage source inverters require some power to switch. So, we utilise controllers to ensure that the DC voltage remains constant and that harmonic currents are dealt with appropriately.

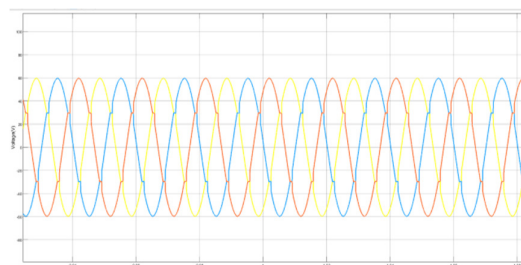


**Fig 12: Source voltage of compensated circuit**

The graph above displays the distorted waveforms of the three-phase source voltage and current within a balanced system featuring a nonlinear load. Fast Fourier Transform (FFT) analysis indicates that the source voltage undergoes distortion as a consequence of the nonlinear behaviour exhibited by the load.

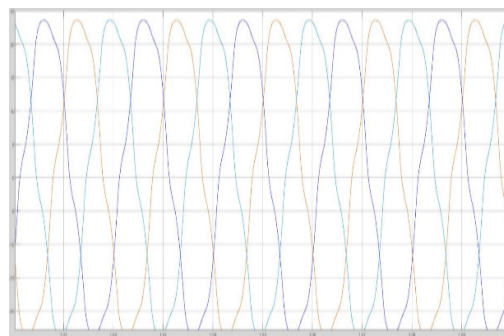


**Fig 13: Source current of compensated circuit**

The graph depicts the distorted waveforms of the source voltage and current in three phases within a balanced system experiencing a nonlinear load. FFT analysis indicates that the nonlinearity of the load leads to distortion in the source current.

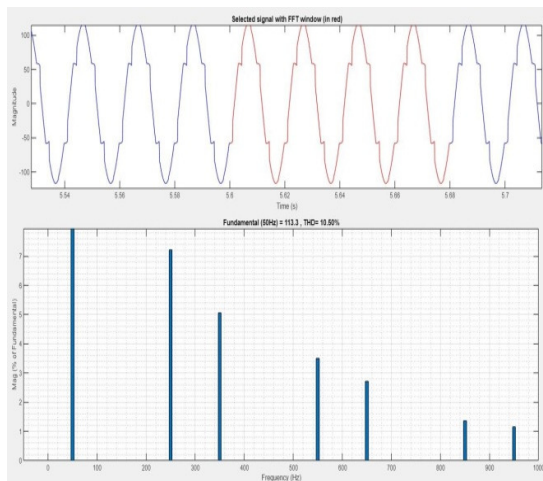


**Fig 14: THD voltage of compensated circuit**

According to the analysis, a PI controller is employed to regulate the total harmonic distortion (THD) of the voltage within the compensated circuit, currently measured at 10.50%. Nevertheless, the implementation of an ANN controller has the potential to further diminish the harmonics present in the waveforms.

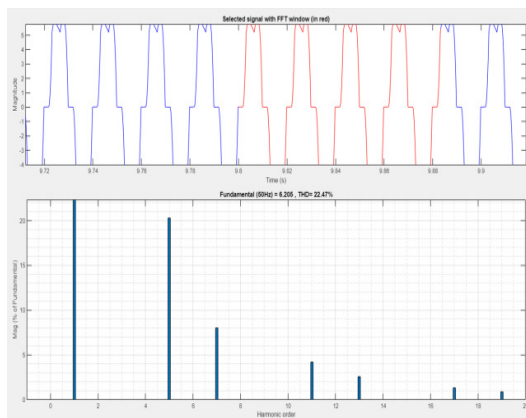


**Fig 15: THD Current for compensated circuit.**

According to the THD analysis above, the compensated circuit's total harmonic distortion (THD) is 7.71%, which is managed by a PI controller. However, the waveforms contain harmonics that can be further reduced by an ANN controller.

**C. Compensated circuit (with ANN-ASF):**

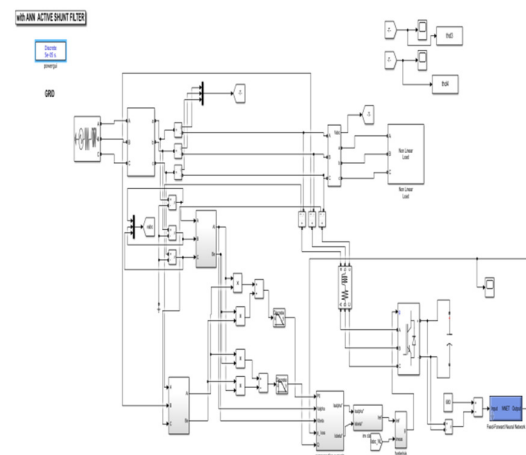


**Fig 16: Simulink Model with ANN Active shunt filter**

The above Simulink model represents the simulation model of Shunt active filter using ANN controller. One crucial aspect of regulating an active shunt filter is maintaining a constant DC voltage on the voltage source inverter's side through intermediate circuit voltage regulation. These filters commonly include a capacitor to store energy. If there is little power flowing between the filter and the AC mains, the capacitor's voltage should remain constant. However, voltage source inverters require some power to switch. So, we utilise controllers to ensure that the DC voltage remains constant and that harmonic currents are dealt with appropriately.



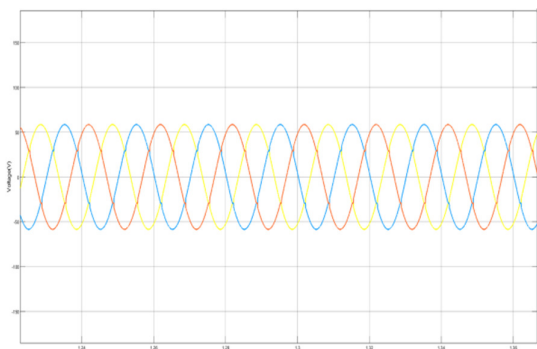


**Fig 17: Source voltage of compensated circuit**

The graph depicts voltage and current waveforms of a three-phase power source in a balanced system with a nonlinear load. To mitigate voltage distortion, ANN control employs Fast Fourier Transform (FFT) analysis.

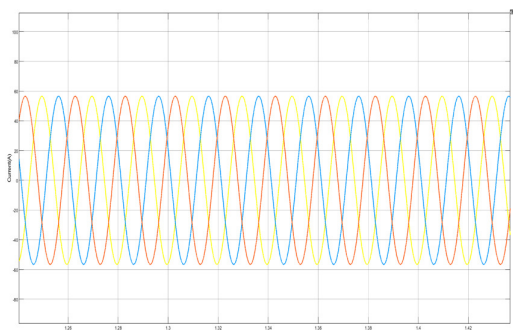


**Fig 18: Source current of compensated circuit**

The graph above showcases the voltage and current waveforms of a three-phase power source within a balanced system affected by a nonlinear load. Utilizing Fast Fourier Transform (FFT) analysis and artificial neural network (ANN) control helps mitigate the distortion observed in the source current.

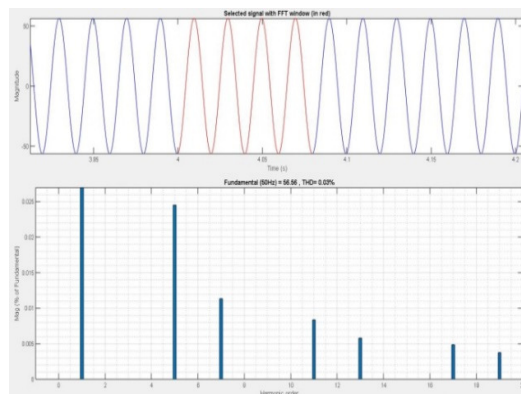


**Fig 19: THD voltage for compensated circuit**

According to the THD analysis above, the adjusted circuit's total harmonic distortion (THD) is 1.89%.

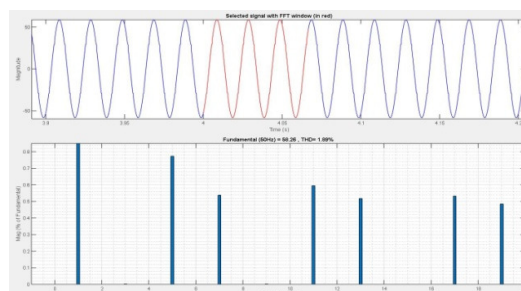


**Fig 20: THD Current for compensated circuit**

According to the THD analysis above, the adjusted circuit's total harmonic distortion (THD) is 0.03%.

**System Parameters:**

parameter	value
voltage	440v
Coupling resistance	1 Ω
Coupling inductance	1 μH
Reference DC voltage	680
Dc link capacitance	1 μF
Frequency	50Hz
Non-linear RL load	10 Ω,380mH

**COMPARISION table of THD without and with active filter:**

PARAMATER	WITHOUT TAF	WITH PI-AF	WITH ANN-AF
VOLTAGE	14.33%	10.50%	1.89%
CURRENT	22.47%	7.71%	0.03%

An Active Shunt filter controller leveraging artificial neural network technology is devised to eliminate harmonics. Detailed in the table above, this controller aims to manage the DC-link voltage and compensate for neutral current, thereby reducing harmonics.

### Conclusion:

The study concludes that employing an artificial neural network (ANN) active filter, overseen by a PQ-based hysteresis controller generating gate pulses for its switching operation, effectively mitigates harmonics in voltage and current waveforms stemming from nonlinear loads. Assessment of harmonic content in the proposed system utilizes instantaneous active and reactive power. Implementation of this system results in a substantial reduction of voltage harmonics from 14.33% to 1.89% and a remarkable decrease in current harmonics from 22.47% to 0.03%.

### References:

1. Nikum, K.; Saxena, R.; Wagh, A. Effect on power quality by large penetration of household non-linear load. In Proceedings of the 2016 IEEE 1st International Conference on Power Electronics, Intelligent Control and Energy Systems (ICPEICES), Delhi, India, 4–6 July 2016; pp. 1–5.
2. Monteiro, F.; Monteiro, S.; Tostes, M.; Bezerra, U. Using True RMS Current Measurements to Estimate Harmonic Impacts of Multiple Nonlinear Loads in Electric Distribution Grids. *Energies* **2019**, *12*, 4132.
3. Witherden, M.S.; Rayudu, R.; Rigo-Mariani, R. The influence of nonlinear loads on the power quality of the New Zealand low voltage electrical power distribution network. In Proceedings of the 2010 20th Australasian Universities Power Engineering Conference, Christchurch, New Zealand, 5–8 December 2010; pp. 1–6.
4. Rakpenthai, C.; Uatrongjit, S.; Watson, N.R.; Premrudeepreechacharn, S. On harmonic state estimation of power system with uncertain network parameters. *IEEE Trans. Power Syst.* **2013**, *28*, 4829–4838.
5. [5] H. Akagi, Y. Kanazawad, and A. Nabae, “Instantaneous power theory and application to power conditioning” IEEE Press, Wiley-inter-science, A Jon Wiley & sons, INC., Publication.
6. [6] M. F. Shousha, S. A. Zaid and O. A. Mahgoub. “Better Performance for Shunt Active Power Filters” Clean electrical Power (ICCEP), IEEE June 2011
7. [7] B. S. Mohammed, K. S. Rama Rao, P. A/L. Nallagownden, “Improvement of power quality of a two-feeder system using Unified Power Quality Conditioner” IEEE Sept 2011
8. Chen, C.-I.; Lan, C.-K.; Chen, Y.-C.; Chen, C.-H. Adaptive Frequency-Based Reference Compensation Current Control Strategy of Shunt Active Power Filter for Unbalanced Nonlinear Loads. *Energies* **2019**, *12*, 3080.
9. IEEE Recommended Practices and Requirements for Harmonic Control in

- Electrical Power Systems. *IEEE Std 519-1992* **1993**
10. Hoon, Y.; Radzi, M.; Amran, M.; Hassan, M.K.; Mailah, N.F. Control algorithms of shunt active power filter for harmonics mitigation: A review. *Energies* **2017**, *10*, 2038.
  11. Pan, D.; Ruan, X.; Bao, C.; Li, W.; Wang, X. Capacitor-Current-Feedback Active Damping with Reduced Computation Delay for Improving Robustness of LCL-Type Grid-Connected Inverter. *IEEE Trans. Power Electron.* **2014**, *29*, 3414–3427.
  12. Liserre, M.; Blaabjerg, F.; Hansen, S. Design and control of an LCL-filter based three-phase active rectifier. In Proceedings of the Conference Record of the 2001 IEEE Industry Applications Conference. 36th IAS Annual Meeting (Cat. No.01CH37248), Chicago, IL, USA, 30 September–4 October 2001; pp. 299–307.
  13. Tang, Y.; Loh, P.C.; Wang, P.; Choo, F.H.; Gao, F. Exploring Inherent Damping Characteristic of LCL-Filters for Three-Phase Grid-Connected Voltage Source Inverters. *IEEE Trans. Power Electron.* **2012**, *27*, 1433–1443.
  14. Wu, W.; He, Y.; Blaabjerg, F. An LLCL power filter for single-phase grid-tied inverter. *IEEE Trans. Power Electron.* **2011**, *27*, 782–789.
  15. Xu, J.; Yang, J.; Ye, J.; Zhang, Z.; Shen, A. An LTCL filter for three-phase grid-connected converters. *IEEE Trans. Power Electron.* **2013**, *29*, 4322–4338.
  16. Anzalchi, A.; Moghaddami, M.; Moghaddasi, A.; Sarwat, A.I.; Rathore, A.K. A new topology of higher order power filter for single-phase grid-tied voltage-source inverters. *IEEE Trans. Ind. Electron.* **2016**, *63*, 7511–7522.
  17. Fang, J.; Li, X.; Tang, Y. A review of passive power filters for voltage-source converters. In Proceedings of the 2016 Asian Conference on Energy, Power and Transportation Electrification (ACEPT), Singapore, 25–27 October 2016; pp. 1–6.
  18. Srivastava, G.D.; Kulkarni, R.D. Design, simulation and analysis of Shunt Active Power Filter using instantaneous reactive power topology. In Proceedings of the 2017 International Conference on Nascent Technologies in Engineering (ICNTE), Navi Mumbai, India, 27–28 January 2017; pp. 1–6.
  19. Swain, S.D.; Ray, P.K.; Mohanty, K.B. Improvement of power quality using a robust hybrid series active power filter. *IEEE Trans. Power Electron.* **2016**, *32*, 3490–3498.
  20. Monroy-Morales, J.; Campos-Gaona, D.; Hernández-Ángeles, M.; Peña-Alzola, R.; Guardado-Zavala, J. An active power filter based on a three-level inverter and 3D-SVPWM for selective harmonic and reactive compensation. *Energies* **2017**, *10*, 297.
  21. Adam, G.; Stan, A.G.; Livint, G. An adaptive hysteresis band current control for three phase shunt active power filter U sing Fuzzy logic. In Proceedings of the 2012 International Conference and Exposition on

- Electrical and Power Engineering, Iasi, Romania, 25–27 October 2012; pp. 324–329.
22. Akagi, H.; Kanazawa, Y.; Fujita, K.; Nabae, A. Generalized theory of instantaneous reactive power and its application. *Electr. Eng. Jpn.* **1983**, *103*, 58–66.
  23. Artemenko, M.Y.; Mykhalskyi, V.M.; Polishchuk, S.Y.; Chopyk, V.V.; Shapoval, I.A. Modified Instantaneous Power Theory for Three-Phase Four-Wire Power Systems. In Proceedings of the 2019 IEEE 39th International Conference on Electronics and Nanotechnology (ELNANO), Kyiv, Ukraine, 16–18 April 2019; pp. 600–605.
  24. Chang, G.W.; Tai-Chang, S. A novel reference compensation current strategy for shunt active power filter control. *IEEE Trans. Power Deliv.* **2004**, *19*, 1751–1758.
  25. Li, Z.; Hu, T.; Abu-Siada, A. A minimum side-lobe optimization window function and its application in harmonic detection of an electricity grid. *Energies* **2019**, *12*, 2619.
  26. Wada, K.; Fujita, H.; Akagi, H. Considerations of a shunt active filter based on voltage detection for installation on a long distribution feeder. *IEEE Trans. Ind. Appl.* **2002**, *38*, 1123–1130.
  27. Maza-Ortega, J.M.; Rosendo-Macías, J.A.; Gomez-Exposito, A.; Ceballos-Mannozi, S.; Barragan-Villarejo, M. Reference current computation for active power filters by running DFT techniques. *IEEE Trans. Power Deliv.* **2010**, *25*, 1986–1995.
  28. Mehra, M.; Pouresmaeil, E.; Akorede, M.F.; Jørgensen, B.N.; Catalão, J.P. Multilevel converter control approach of active power filter for harmonics elimination in electric grids. *Energy* **2015**, *84*, 722–731.
  29. Kanjiya, P.; Khadkikar, V.; Zeineldin, H.H. A noniterative optimized algorithm for shunt active power filter under distorted and unbalanced supply voltages. *IEEE Trans. Ind. Electron.* **2012**, *60*, 5376–5390.